DESIGN OF MULTI-PROPELLANT STAR GRAINS FOR SOLID PROPELLANT ROCKETS

S. KRISHNAN & TARIT K. BOSE
Department of Aeronautical Engineering
Indian Institute of Technology, Madras-600036

(*Received* 29 *November* 1976; *revised* 24 *July* 1979)

A new approach to solve the geometry-problem of solid propellant star grains is presented. The basis of the approach is to take the web-thickness (a ballistic as well as a geometrical property) as the characteristic length. The nondimensional characteristic parameters representing diameter, length, slenderness-ratio, and ignitor accommodation of the grain are all identified. Many particular cases of star configurations (from the configurations of single propellant to those of four different propellants) can be analysed through the identified characteristic parameters. A better way of representing the single-propellant-star-performance in a design graph is explained. Two types of dual propellant grains are analysed in detail. The first type is characterised by its two distinct stages of burning (initially by single propellant burning and then by dual propellant burning); the second type has the dual propellant burning throughout. Suitability of the identified characteristic parameters to an optimisation study is demonstrated through examples.

When simplicity, reliability, development time and cost are the most important factors, the star configuration is one of the commonly opted geometries. Typical applications of star grains include tactical and sounding rockets, and satellite launch vehicles[1–4]. Even in large high performance segmented grains, sometimes star configuration is used for some of the segments[5]. Although from mechanical behaviour point of view the wagon-wheel grains are sometimes superior to star grains, they usually do not give a web as thick as star grains. The finocyl-configuration, which is a widely used one for high performance grains, is only a variation of the classical star.

The overall design of any cylindrical grain involves two major steps : (1) development of a system of equations to represent the burning and port areas of the different portions of grain (head end, cylindrical portion, and nozzle end), and (2) optimising the grain geometry for the imposed constraints. The step (2) is carried out mostly through high speed computing machines[6,7]. However, to know clearly the effects from the different portions of grain it is usual to study the performance of the portions separately through the equations developed in step (1). In this kind of study, the study of cylindrical portion is of special importance because the cylindrical portion forms the major part of grain in many cases, and so the results obtained qualitatively represent the performance of entire grain.

Stone[8], Vandenkerckhove[9], and Barrere *et al.*[10] analysed the single propellant star grain cross sections. The main objection in the use of single propellant star grain is the propellant sliver. A cross section of multiple propellants of different burning rates can be used to avoid sliver. Towards this concept a dual propellant (or bipropellant) star grain cross section was first analysed by Rogers [11] and subsequently by Barrere and Larue[12,13]. All these studies, on one aspect or the other, analyse only particular cases of configurations. Further the non-dimensional characteristic parameters that meaningfully represent the important properties of grain have not been fully identified. Also the important dual propellant configurations have not been completely analysed. Therefore the present study, by considering a general star grain cross section of four different propellants and obtaining a system of characteristic parameters, aims to remove these gaps.

NOTATIONS

A = non-dimensional parameter of initial port area, Ap_i/w^2
Ab = burning surface area
Ap_i = initial port area
D = grain diameter
f = fillet ratio, r/l

J = ratio of nozzle throat area to port area
k = ratio of burning rate of a propellant to that of propellant C
L = straight through grain length
l = linear dimension
m = ratio of density of a propellant to that of propellant C
$\dot{m}$ = mass burning rate
n = number of star points
R = non-dimensional root radius, Rm/w
R_m = root radius
r = fillet radius; linear regression rate
S = non-dimensional burning perimeter, s^E/w
s = burning perimeter
sE = equivalent burning perimeter
w = burning web thickness
y = non-dimensional parameter, w/l
y^* = web ratio, w/w_1
y^*_R = reference web ratio

Greek letters

Γ = surface ratio, $s_y{}^{E*}/s_y{}^{E*R}$
δ = maximum percentage deviation from the specified Γ—trace
ϵ = angular fraction
η_l = loading fraction
η_s = sliver fraction
Θ = $\theta/\bar{\theta}_N$
θ = star opening angle
θ_N = star opening angle of neutral burning single propellant grain
Λ = non-dimensional parameter of L/D ratio, Eq. (9)
ν = ratio of single-propellant-web to w_1
ρ = propellant density
Φ = non-dimensional parameter of diameter, Eq. (7)

Subscripts

A, B, C and D = for propellants A, B, C and D respectively
b = burnout condition
f = conditions at which η_s just becomes zero
N = neutral burning condition
0 = at $y^*=0$
1 = at $y^*=1$; for propellant A
2 and 3 = for the propellants B and D respectively

ANALYSIS

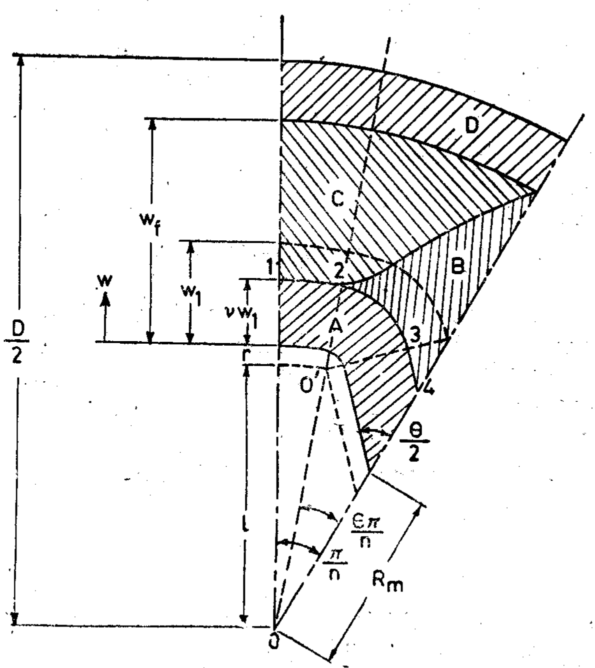

Fig. 1—Sector of internal burning star with multiple propellants.

General Grain Cross Section

The sector of star grain with multiple propellant compositions considered for the analysis is shown in Fig. 1. The propellants A, B, C and D can have different burning rates (r_A, r_B, r_C and r_D respectively) and densities (ρ_A, ρ_B, ρ_C and ρ_D respectively). A constraint on the burning rates of B and C is that the burning rate of B is faster than that of C. The propellant A has web thickness of νw_1 where w_1 is the web at which the straight star point just vanishes; also $\nu \leqslant 1$. The web thickness at which the propellant sliver becomes zero is denoted as w_f. For the general cross section shown in Fig. 1, at the burnout of B and C $w = w_f$.

The following assumptions are made for the general star grain cross section : (1) any point on the burning surface moves perpendicular to the tangent plane at that point; (2) the burning rate though each propellant is same at any point on the burning perimeter at a given instant of time; (3) erosive burning effects are negligible; and (4) the propellants are not insulated from each other.

From the considered general configuration shown in Fig. 1, many particular configurations can be obtained. For example the single propellant star configuration is obtained when $k_1 = k_2 = m_1 = m_2 = 1$; in this case y_f tends to infinity indicating η_s is never equal to zero for the single propellant grain. Similarly the dual propellant configuration considered by Rogers[11] is obtained when $\nu = 0$, $m_2 = m_3 = k_3 = 1$ and $\epsilon = 1$.

The generalised characteristic equations of equivalent burning perimeter and port area for all the four phases of burning are given in literature[16].

Non-dimensional Characteristic Parameters

In the case of multiple propellant composition the mass flow rate of combustion products per unit length of grain, say when B and C are burning, is:

$$\dot{m}_{BC} = r_C \, \rho_C \, (k_2 \, m_2 \, s_B + s_C) = r_C \, \rho_C \, S^E_{BC}$$

where

$$k_2 = r_B/r_C$$
$$m_2 = \rho_B/\rho_C \qquad (1)$$

and, s_B and s_C are the physical burning perimeters of propellants B and C respectively; here the propellant C has been taken as the reference. Similarly when the propellant A or D is burning,

$$\dot{m}_A = r_C \, \rho_C \, (k_1 \, m_1 \, s_A) = r_C \, \rho_C \, S^E_{S_A}$$

where

$$k_1 = r_A/r_C \qquad (2)$$
$$m_1 = \rho_A/\rho_C$$

or

$$\dot{m}_D = r_C \, \rho_C \, (k_3 \, m_3 \, s_D) = r_C \, \rho_C \, S^E_D$$

where

$$k_3 = r_D/r_C \qquad (3)$$
$$m_3 = \rho_D/\rho_C$$

Here S^E_{BC}, S^E_A and S^E_D are termed as equivalent burning perimeters. In the case of single propellant grains, during the presence of star the star opening angle, θ required for neutral burning depends only on the number of star points, n. Denoting this as $\overline{\theta}_N$ we define

$$\Theta = \theta/\overline{\theta}_N \qquad (4)$$

the length l being the major dimension of mandrel r/l (denoted as f) is taken as one of the geometrical properties of grain.

For the selected propellant and nozzle-configuration, the required thrust-time trace can be transformed to burning area-burnt distance (A_b—w) trace. This means that the final web thickness of the grain to be designed is approximately known[14]. Therefore, rather than D as in Ref. 8 or l as in Ref. 9 & 10, w becomes a better suited characteristic length for non-dimensionalisation[15]. This idea of using w as the characteristic length is employed in the present work. The required A_b—w trace can be effectively defined by specifying A_b at some suitable burnt distances. Towards this objective the non-dimensional burnt distance is defined as

$$y^* = w/w_1 \qquad (5)$$

Also we define the surface ratio as

$$\Gamma = s^E_{y^*} \Big/ s^E_{y^*_R} \qquad (6)$$

where $S^E_{y^*}$ is the equivalent burning perimeter at y^* and $S^E_{y^*_R}$ is the equivalent burning perimeter at the reference y^*_R.

Denoting w/l as y, and s^E/w as S for the web w, the diameter of grain cross section (D) and the length of straight-through grain (L) can be written as,

$$D = 2w\,[(1 + f + y)/y] = 2\,w\Phi \tag{7}$$

$$L = A_b/(Sw) \tag{8}$$

Therefore Φ (or y if f is specified) and S represent the diameter of cross section and the length of straight-through grain respectively. For the straight-through grain L/D ratio can be written as

$$L/D = \Lambda\, A_b/(2w^2)$$

where

$$\Lambda = y/[S(1 + f + y)] \tag{9}$$

It follows that Γ can be taken to represent the L/D ratio of grain. Similarly A_{pi}/w^2 (denoted as A) and R_m/w (denoted as R) represent the throat to port area ratio (J) and the initial core available for igniter respectively. The other two important design parameters are : (1) loading fraction η_l which is defined as the ratio of initial propellant volume to motor volume, and (2) sliver fraction η_s which is defined as the ratio of propellant volume at burnout to total initial propellant volume.

The four phases of burning that can be identified for the cross section are : (1) $0 \leqslant y^* \leqslant v$ (2) $v \leqslant y^* \leqslant 1$, (3) $1 \leqslant y^* \leqslant y_f^*$, and (4) $y_f^* \leqslant y^*$.

RESULTS AND DISCUSSIONS

Single Propellant Grains

The resulting equations of the characteristic parameters are functions of y, ϵ, n, Θ and f. Although an analytical solution is not obtainable for any specified value of a characteristic parameter, the equations readily lead themselves to common iterative procedures. For the present study, with ϵ and η_l as x and y coordinates, design graphs were drawn for all combinations of : $n=5$ and 7; $\Theta = 0.9$, 1.0 and 1.1; $f = 0.08$ and 0.12[16]. As a representative set, the design graphs for $n=7, f=0.12$, and $\Theta=0.9$ are shown in Figs. 2

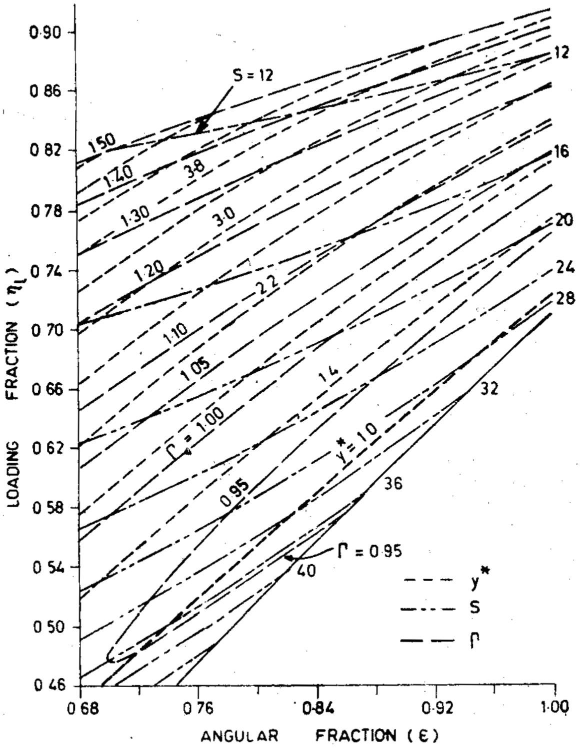

Fig. 2—Design graph for single propellant star grain with parametric values of y^*, S and Γ; $n=7$, $f=0.12$ and $\Theta=0.9$.

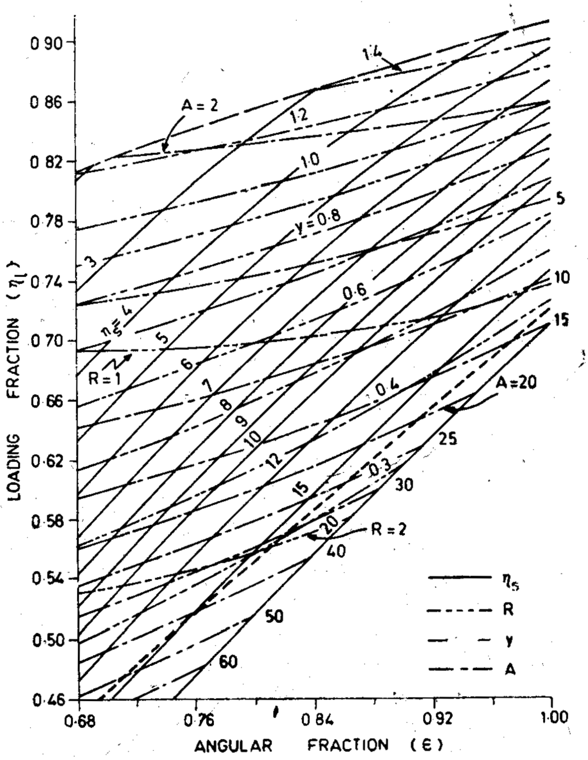

Fig. 3—Design graph for single propellant star grain with parametric values of y, η_s, A and R; $n=7, f=0.12$ and $\Theta=0.9$.

and 3. For the surface ratio, Γ the initial grain surface at $y^*=0$ is taken as the reference. The upper and lower boundaries of the graphs are by $\Gamma=1.5$ and $\eta_s=20$ per cent respectively.

With any parametric quantity as a constraint, the values of the other characteristic parameters can be directly read from the graph. For the known web thickness, y represents the grain diameter, Eq. (7); for the given burning area and web thickness, S represents grain length, Eq. (8). So the often imposed condition of constant grain diameter or constant grain length can be conveniently handled by choosing the appropriate parametric curve.

For the given A_b—w trace with some acceptable deviations, the graphs readily demonstrate the following points in the design of straight through grains : (i) high loading fraction, ηl implies high L/D ratio;, (ii) ηl can be raised by increasing ϵ and by decreasing n, Θ, and f (stress concentration is also raised in this process[17]); (iii) sliver fraction can be reduced by increasing n and by reducing ϵ, Θ and f.

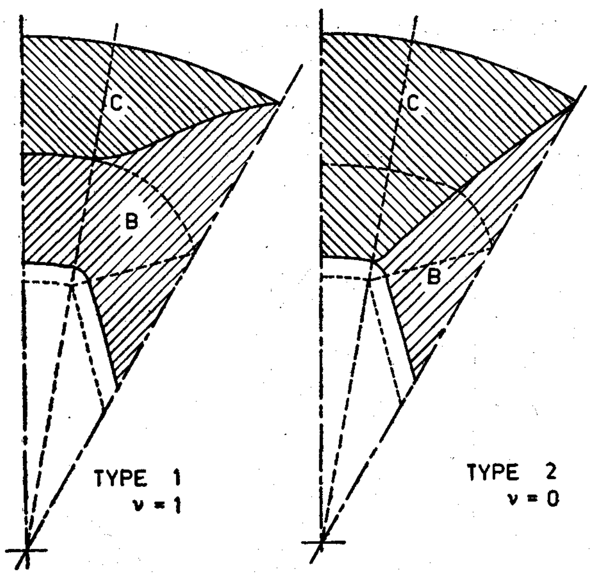

Fig. 4—Dual propellant grains.

Dual Propellant Grains

Many multipropellant configurations can be analysed through the considered grain-cross-section. However, only the two dual-propellant types shown in Fig. 4 are analysed here. In the first type $v=1$, $k_1=k_2$, $m_1=m_2=1$, and $D=2\,w_f\ (1+f+y_f)/y_f$; in the second the only difference is $v=0$. For the purpose of comparison the frequently desired neutral burning condition is chosen. In the case of type 1, when $\epsilon<1$ the surface trace is not continuous at $y^*=1$. Therefore to solve for the conditions of neutrality Γ of $0\leqslant y^*\leqslant 1$ has $s^E{}_B$ at $y^*=0$ as the reference and Γ of $1\leqslant y_f^*\leqslant 1$ has $s^E{}_{BC}$ at $y^*=1$ as the reference. Due to the possibility of discontinuity in the Γ—trace at $y^*=1$ we define Γ_t as the ratio of equivalent burning perimeters of successive phases at $y^*=1$. Then for the grain of type 1,

$$\Gamma_t = (s^E{}_{BC}/s^E{}_B)\ y^*=1$$

In the case of type 2 for the entire range of $0\leqslant y^*\leqslant y_f^*$, Γ is continuous and has the initial burning perimeter $(s^E{}_{BC})_o$ as the reference. The condition of neutrality ($\Gamma=1$) is specified only at $y^*=1$ and $y^*=y_f^*$. In any given phase of multipropellant burning the Γ— trace is not unimodal between the end points, However mainly to simplify the problem we have imposed the condition of neutrality only at two points., i.e., at $y^*=1$ and $y^*=y_f^*$. The equations of surface ratios are functions of n, ϵ, f, Θ and k_2. For the parametric values of n, ϵ and f the equations can be simultaneously solved for burning rate ratio and Θ. We denote the burning rate ratio of neutral burning as $k_{2,N}$.

Type 1

From the specified neutral burning conditions and n, for the dual propellant grain of type 1 it can be easily shown through the resulting equations that $k_{2,N}$ and Γ_t are independent of f. However for the number of star points $n\leqslant 5$, the compatibility range of ϵ ($R_m\geqslant 0$) depends upon f. This is marked by the termination of the curves $n=4$ at the asterisks in Figs. 5 and 6; the corresponding value of $f=0.1$. The variation of $k_{2,N}$ with ϵ for different number of star points is shown in Fig. 5; evidently Θ_N is unity for all n. When ϵ is less than unity a sudden drop in the equivalent burning perimeter occurs at $y^*=1$ and

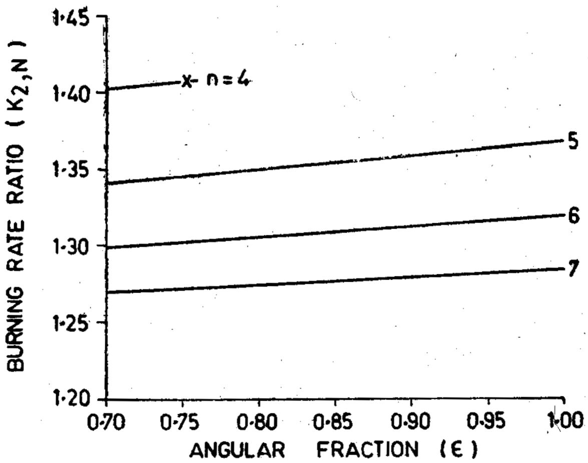

Fig. 5—Burning rate ratio requirement for near neutral burning dual propellant grains; $\nu=1$ & $f=0.1$.

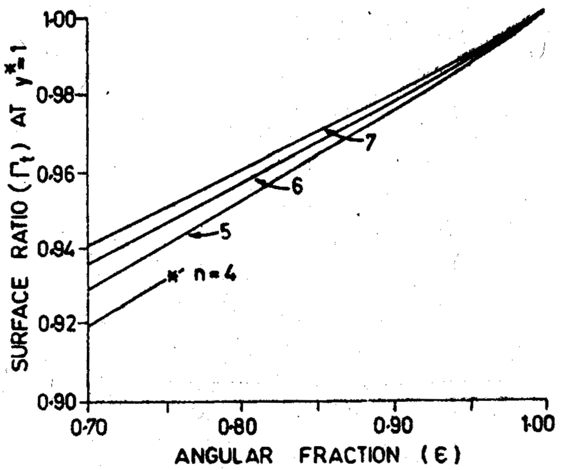

Fig. 6—Variation of surface ratio at transit (Γ_t) for near neutral burning dual propellant grains; $\nu=1$ and $f=0.1$.

the related quantity, Γ_t is shown plotted in Fig. 6. Typical surface ratio traces for $n=5$ and 7 are shown in Fig. 7. Considering only the second phase of burning, it is seen that the deviation from neutrality ncreases with the increase in ϵ and the decrease in n.

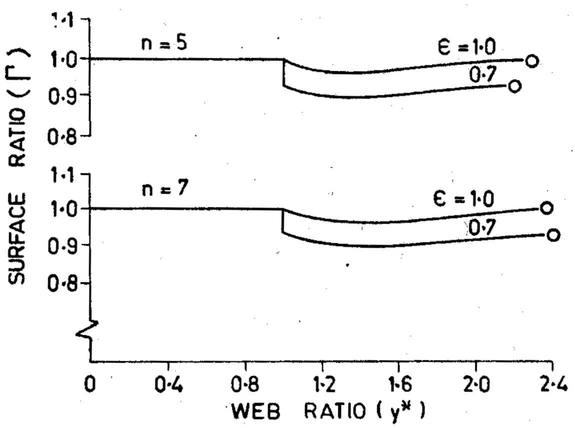

Fig. 7—Comparison of surface ratio variation of near neutral burning dual propellant grains; $\upsilon = 1$ and $f=0.1$.

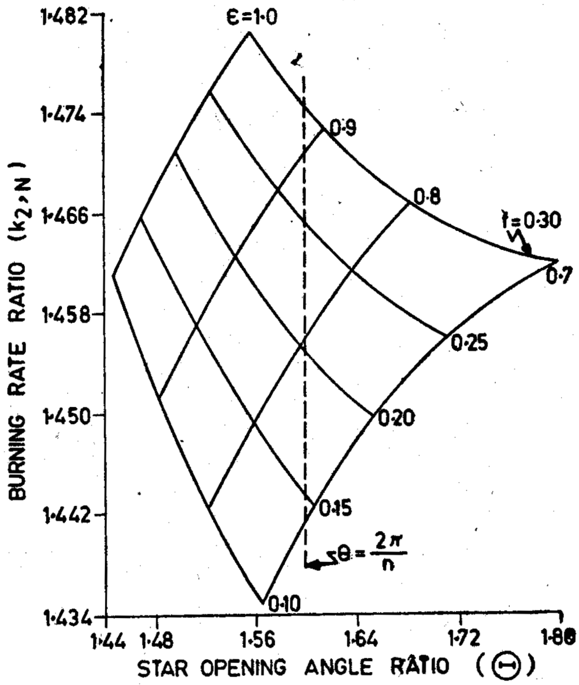

Fig. 8—Conditions of neutral burning for the four pointed dual propellant grain; $\upsilon=0$ and $n=4$.

Type 2

The characteristics of the neutral burning grains of type 2 were calculated from $n=4$ to 7. Fig. 8 shows the typical conditions of neutral burning grain of $n=4$; the vertical dotted line in the figure represents the 'slotted star' ($\theta=2\pi/n$). At higher values of n it is noted : (1) for the given change in f, the variation required on $k_{2,N}$ is less while that on Θ_N is more, and (2) particularly at high f, $k_{2,N}$ remains essentially constant for a wide variation in ϵ. Fig. 9 presents the surface ratio traces for $n=5$. Though the traces have only small deviations from neutrality, they depict the multimodal nature of surface area variation

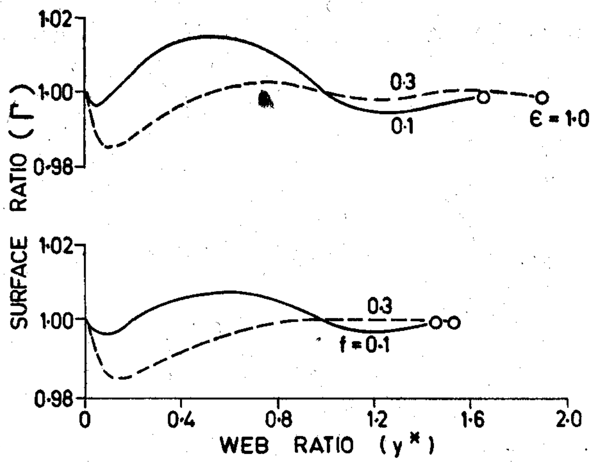

Fig. 9—Comparison of surface ratio variation of near neutral burning dual propellant grains; $\nu = 0$ and $n=5$.

Comparison

Table 1 gives the typical performance values of the two grain types. The important comparative points are, in type 1 : (i) $k_{2,N}$ is less; (ii) the loading fraction and therefore the L/D ratio are higher; (iii) the deviation from neutral burning condition, δ is more; (iv) the variation of $y_f{}^*$ with ϵ at low values of f is less—this means that the ratio of webs in the second and first phases of burning remains essentially constant. In

TABLE 1

PERFORMANCE VALUES FOR THE COMPARISON OF NEUTRAL DUAL PROPELLANT GRAINS

Type	n	ϵ	f	$-N$	$k_{2,N}$	ηl	ϕ	Λ	A	R	Γ_t	δ
1	5	0.7	0.3	1.000	1.342	0.652	2.836	0.0198	8.789	1.102	0.929	$^{+0}_{-4.30}$
	5	0.7	0.1	1.000	1.342	0.812	2.211	0.0325	2.887	0.433	0.929	$^{+0}_{-4.30}$
	5	1.0	0.1	1.000	1.369	0.966	1.799	0.0492	0.345	0.021	1.000	$^{+0}_{-5.40}$
	7	1.0	0.1	1.000	1.286	0.865	2.060	0.0375	1.798	0.449	1.000	$^{+0}_{-4.83}$
2	5	0.7	0.3	1.772	1.401	0.539	3.697	0.0116	19.820	2.021	1.000	$^{+0}_{-1.54}$
	5	0.7	0.1	1.520	1.374	0.672	2.982	0.0179	9.117	1.168	1.000	$^{+0.80}_{-0.48}$
	5	1.0	0.1	1.419	1.390	0.878	2.288	0.0304	2.003	0.406	1.000	$^{+1.50}_{-0.48}$
	7	1.0	0.1	1.381	1.307	0.751	2.669	0.0223	5.573	0.998	1.000	$^{+1.00}_{-0.46}$

type 2 for the given n and surface trace, Θ is not fixed. Therefore the suitable value of Θ satisfying both ballistic and mechanical properties can be found easily. In the present work no study is made to compare the mechanical behaviour of the two configurations. However, for the given chamber pressure it is likely that the debonding tendency at the interface between the two propellants is less for the type 1. In both the types, (i) as noted in single propellant grain η_l can be raised by increasing ϵ and by decreasing $_n$ and f, (ii) with the increase in n, $k_{2,N}$ reduces, and (iii) for the given n a wide variation in ϵ results only in a small change in $k_{2,N}$.

The configuration of slotted star ($\theta=2\pi/n$) is of interest in many applications. For the dual propellant slotted stars of $\epsilon=1$ and $\nu=0$, through the surface-area traces obtained, Barrere and Larue[12] concluded that neutral burning cannot be obtained for $n>5$. The basic reason for this behaviour readily follows from the present study : for any dual-propellant phase to be neutral the corresponding single propellant phase should be progressive. Evidently the slotted stars of $n>5$ do not satisfy this condition of neutrality since their values of Θ are all less than unity. For $n>5$ the single propellant slotted stars have regressive burning in the first phase and the usual progressive burning in the second phase. Therefore the frequently desired booster-sustainer combination can be easily obtained in slotted stars through either of the dual propellant types that we have discussed. The typical Γ—trace of the basic single propellant slotted star and the modified traces of booster-sustainer combination by the dual propellant compositions are shown in Fig. 10.

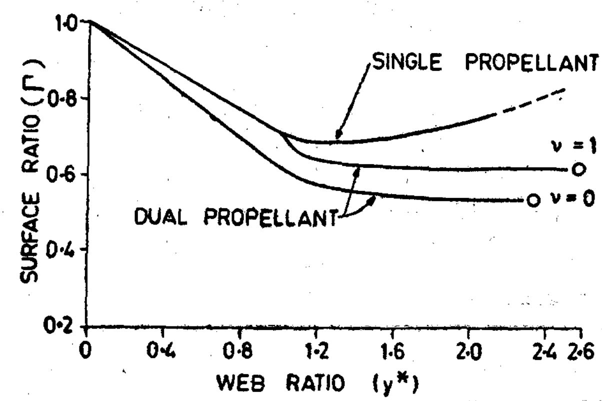

Fig. 10—Booster-sustainer combination in dual propellant grains; $n=8$, $\theta=\pi/4$, $\epsilon=1$, $f=0.1$ and $k_2=1.3$.

Grain Optimisation

To optimise the configuration, the characteristic equations of the different portions of grain are suitably coupled under the imposed constraints. However, to demonstrate that the identified characteristic parameters are readily amenable to optimisation study, we have chosen here two examples of straight-through-grain design. The details of the problems and the results are given in Tables 2 and 3; the

TABLE 2

DETAILS OF THE OPTIMISATION STUDY OF SINGLE PROPELLANT GRAINS

Problem

Aim	: Minimise sliver fraction, η_s
Constraints	: Single propellant star, n=4, 5, 6, 7 or 8; $f \geqslant 0.1$; $\eta_l \geqslant 0.75$ Grain length : $S \geqslant 13.35$; Grain diameter : $\varphi \leqslant 2.719$; Throat-to-port area ratio, J: $A \geqslant 3$; Igniter accommodation: $R \geqslant 0.3$; Γ—trace : $\Gamma=0.95$, $\Gamma_t=1.05$

Solution

n	ϵ	f	Θ	η_s	η_l	y_b	y_b^*	S	φ	Λ	A	R
4	0.572	0.1	0.909	0.0661	0.750	0.649	1.700	17.10	2.694	0.02170	5.70	0.351
5	0.677	0.1	0.914	0.0708	0.750	0.643	1.742	17.22	2.710	0.02143	5.77	0.559
6	0.777	0.1	0.918	0.0748	0.751	0.640	1.775	17.28	2.719	0.02128	5.77	0.702
7	0.876	0.1	0.922	0.0785	0.755	0.640	1.800	17.29	2.719	0.02127	5.70	0.802
8	0.970	0.1	0.925	0.0817	0.758	0.640	1.822	17.30	2.179	0.02126	5.63	0.881

TABLE 3

DETAILS OF THE OPTIMISATION STUDY OF DUAL PROPELLANT GRAINS

Problem

Aim	: Maximise the loading fraction, η_l
Constraints	: Dual propellant star, Type 1 or Type 2; n=4, 5, 6 or 7; $f \geqslant 0.1$; $\eta_s = 0$; $k_2 \leqslant 1.6$; Grain length : $S \geqslant 13.35$; Grain diameter: $\Psi < 2.719$; Throat-to-port area ratio, J : $A \geqslant 3$; Igniter accommodation: $R \geqslant 0.3$; Γ—trace: $0.98 \leqslant \Gamma 1 \leqslant 1.02$, $0.98 \leqslant \Gamma_f \leqslant 1.02$, Γ—trace to be continuous (therefore for type 1 configuration $\epsilon = 1$), $1.4 < y^*_f < 3.0$.

Solution

Type	n	ϵ	f	..	k_2	η_1	y_f	y^*_f	S	Φ	Λ	A	R	δ[a]
1[b]	6	1.000	0.242	1.038	1.350	0.810	1.000	2.724	14.09	2.242	0.0316	3.000	0.570	+0 −2.0
	7	1.000	0.162	1.033	1.314	0.810	0.936	2.469	14.10	2.242	0.0316	3.000	0.631	+0 −1.8
2	4	0.998	0.209	1.823	1.566	0.843	0.825	1.400	15.50	2.465	0.0262	3.000	0.499	+1.7 −0
	5	1.000	0.108	1.577	1.448	0.841	0.763	1.400	15.41	2.451	0.0265	3.000	0.579	+0.6 −0
	6	1.000	0.100	1.292	1.312	0.832	0.796	1.778	14.98	2.383	0.0280	3.000	0.604	+0 −0.3
	7	1.000	0.100	1.232	1.257	0.791	0.753	1.889	15.46	2.461	0.0263	3.991	0.789	+0 −0.2

[a] Acceptable variation of Γ taken as 0.98 to 1.02 for the entire range of y^*.
[b] n=4 infeasible due to the constraints on A, R and S; n=5 infeasible due to the constraint on A.

sequencial unconstrained minimisation technique (SUMT) was used for the resulting nonlinear equations of the objective function and the constraints[18].

CONCLUSIONS

As compared to the earlier work the basic new element of this study is the consideration of web thickness as the characteristic length to identify the characteristic parameters, representing the usually specified constraints in grain-design. As the identified parameters are quite general in nature they can be used also for other grain types.

The types of design graphs obtained for the single propellant star offer much wider information than the available ones. Grain designs are never finalised through graphs. Yet these graphs enable choosing a good starting point for the optimisation study.

The type 1 dual propellant grain usually gives a higher loading fraction but its surface trace deviation is more. Also it has a step in its surface trace when $\epsilon < 1$. However, this property can be advantageously used to obtain dual thrust traces. When the surface trace and n are fixed for a dual propellant grain, a wide variation in geometrical properties results only in a small change in k_2. Therefore the possible deviation on k_2 due to practical limitations should be carefully considered for the actual performance deduction of grain.

The characteristic parameters and their equations are readily amenable to grain optimisation studies.

ACKNOWLEDGEMENT

The help of Professor P. Venkata Rao and Dr. V.V. Sastry of the Department of Electrical Engineering in carrying out the grain optimisation study is gratefully acknowledged. Many thanks are also due to Mr. Rajaram Nagappa of Vikram Sarabhai Space Centre, Trivandrum, and Major Raghavan and Mr. C.S. Bhatnagar of Defence Research and Development Laboratory, Hyderabad; author S. Krishnan had very useful discussion and many private communications with them.

REFERENCES

1. TAYLOR, W.R.J., 'Jane's All the World's Aircraft 1965-66' (Samson-Low, Marston and Co., London), 1965, p. 503.
2. FURST, J.W., *J. Br. Interplanetary Soc.*, **25** (1972), 153.
3. ROLFE, J.A., *J. Br. Interplanetary Soc.*, **26** (1973), 7.
4. ANON., *SLV Project Bull. Indian Space Res. Org.*, **1** (1975), 2.
5. ZIMMERMAN, C.A., 'Status of the United States Large Solid Rocket Motor Program' (17th Int. Aeronaut. Congr., Madrid), 1966.
6. VELLACOTT, R.J. & CAVENY, L.H., 'A Computer Program for Solid Propellant Rocket Motor Design and Ballistic Analysis'. (Am. Rocket Soc., Pap), 1962, p. 2315-62.
7. GORNEY, L.J., 'A Generalized Approach to Rapid Evaluation of Solid Propellant Grain Geometries' (Am. Rocket Soc., Pap), 1962, p. 2316-62.
8. STONE, M.W., *Jet Propulsion*, **28** (1958), 236.
9. VANDENKERCKHOVE, J.A., 'Internal Burning Star and Wagon Wheel Designs for Solid Propellant Grains', USAF-ARDC contract S. 61 (052) 58-13, Publication de l' Institut d' Aeronautique, Universite Libre de Bruxelles, 1958.
10. BARRERE, M., JAUMOTTE, A., VEUBEKE, B.F. & VANDENKERCKHOVE, J.A., "Rocket Propulsion" (Elsevier Publishing Co., Amsterdam), 1960, p. 301.
11. ROGERS, K.H., 'Mathematical Design of a Sliverless Rocket Engine ' (Am. Rocket Soc., Pap), 1961, p. 1616-61.
12. BARRERE, M. & LARUE, P., *La Recherche Aeronautique*, **91** (1962), 33.
13. WILLIAMS, F.A., BARRERE, M., & HUANG, N.C., 'Fundamental Aspects of Solid Propellant Rockets' (Agardograph No. 116, Technivision Services., Slough), 1969, p. 230.
14. 'Solid Rocket Motor Performance Analysis and Prediction', NASA SP-8039, 1971.
15. KRISHNAN, S., *J. Spacecraft and Rockets*, **12** (1975), 60.
16. KRISHNAN, S., 'Certain Design Aspects of Solid Propellant Rocket Motors' Ph.D. Thesis, (Indian Inst. of Technol., Madras), 1976.
17. ORDAHL, D.D. & WILLIAMS, M.L., *Jet Propulsion*, **27** (1957), 657.
18. KUESTER, J.L. & MIZE, J.H., 'Optimization Techniques with Fortran' (McGraw-Hill Book Co., New York), 1973 p. 412,